ORIGINAL ARTICLE

A Novel Model System for Design of Biomaterials Based on Recombinant Analogs of Spider Silk Proteins

Vladimir G. Bogush · Olga S. Sokolova ·
Lyubov I. Davydova · Dmitri V. Klinov ·
Konstantin V. Sidoruk · Natalya G. Esipova ·
Tatyana V. Neretina · Igor A. Orchanskyi ·
Vsevolod Yu Makeev · Vladimir G. Tumanyan ·
Konstantin V. Shaitan · Vladimir G. Debabov ·
Mikhail P. Kirpichnikov

Abstract Spider dragline silk possesses impressive mechanical and biochemical properties. It is synthesized by a couple of major ampullate glands in spiders and comprises of two major structural proteins—spidroins 1 and 2. The relationship between structure and mechanical properties of spider silk is not well understood. Here, we modeled the complete process of the spider silk assembly using two new recombinant analogs of spidroins 1 and 2. The artificial genes sequence of the hydrophobic core regions of spidroin 1 and 2 have been designed using computer analysis of existing databases and mathematical modeling. Both proteins were expressed in *Pichia pastoris* and purified using a cation exchange chromatography. Despite the absence of hydrophilic N- and C-termini, both purified proteins spontaneously formed the nanofibrils and round micelles of about 1 μm in aqueous solutions. The electron microscopy study has revealed the helical structure of a nanofibril with a repeating motif of 40 nm. Using the electrospinning, the thin films with an antiparallel β-sheet structure were produced. In summary, we were able to obtain artificial structures with characteristics that are perspective for further biomedical applications, such as producing three-dimensional matrices for tissue engineering and drug delivery.

V. G. Bogush (✉) · L. I. Davydova · K. V. Sidoruk ·
V. Y. Makeev · V. G. Debabov
State Scientific Center "GosNIIGenetika",
1, 1-st Dorozhny proezd,
113545 Moscow, Russia
e-mail: bogush@genetika.ru

O. S. Sokolova · I. A. Orchanskyi · K. V. Shaitan ·
M. P. Kirpichnikov
Faculty of Biology, Department of Bioengineering,
Moscow State University,
1 Leninskie Gory, Bld 12,
119991 Moscow, Russia

O. S. Sokolova
Institute of Biochemistry, RAS,
33 Leninsky ave, Bld 2,
119071 Moscow, Russia

D. V. Klinov · T. V. Neretina
Institute of Bioorganic Chemistry, RAS,
16/10 Miklukho-Maklaya St,
117997 Moscow, Russia

N. G. Esipova · V. G. Tumanyan
Engelhardt Institute of Molecular Biology, RAS,
32 Vavilova St,
Moscow 119991, Russia

Abbreviations
PPII   poly-L-proline
FTIR   Fourier transform infrared spectroscopy

Introduction

Spider dragline silk features impressive mechanical properties. Its tensile strength is approaching that of steel (Cunniff et al. 1994), while the extensibility is similar to rubber (Vehoff et al. 2007). Due to these unique properties and availability of genetic tools for sequence manipulation, interest to the spider dragline silk rose significantly during the past decade.

A special interest has emerged recently for the use of spider silk in various biomedical applications due to its biocompatibility and ability to biodegrade. The synthetic porous three-dimensional matrices are produced by electrospinning (Ayutsede et al. 2005) or chemically (Tamada 2005) form the analogs of the extracellular matrix. Such matrices can be used for tissue engineering to produce the artificial bones, skin, or ligaments (Jayaraman et al. 2004; Kim et al. 2005; Min et al. 2004; Hoffman et al. 2007). Spider silk may also be used as nanocomposite, in complex with nanoparticles (biosilicone) of Si dioxide (Po Foo et al. 2006), Ti dioxide (Feng et al. 2007), and hydroxyapatite (Furuzono et al. 2004). Recently, a successful utilization of the nanocomposites as the nanocontainers for controlled drug and gene delivery and release was demonstrated (Fang et al. 2006; Katti et al. 2004; Hoffman et al. 2007).

The unique mechanical and biochemical properties of spider silk are caused by its molecular structure. Spider dragline silk contains crystalline regions embedded in a less organized "amorphous" matrix. It is synthesized by a couple of major ampullate glands of spider and consists of two major structural proteins—spidroins 1 and 2 (Xu and Lewis 1990; Hinman and Lewis 1992). The spidroins as well as the structural proteins of *Bombix mori*—fibroins—belong to the self-assembling fibrous proteins. Under native conditions (e.g., inside the spider's spinning gland), they form complex structures—the silk fibrils. Under the in vitro conditions, they assemble to the less complex structures, the nanofibrils (Oroudjev et al. 2002; Slotta et al. 2007).

Natural spidroins 1 and 2 of a *Nephila's* dragline are large proteins with the molecular weight of 275 and 320 kDa, respectively. They exhibit a periodic pattern in the core part of the molecule and possess unique non-periodic hydrophilic domains on the N- and C-termini.

Each initial repeat contains a hydrophobic poly-Ala (poly-A) segment which is four to nine amino acid residues long and a hydrophilic Gly-enriched segment. The most abundant Gly-rich motif in spidroin 1 is Gly-Gly-X, where "X" denotes Tyr, Leu, Ala, or Gln (Xu and Lewis 1990). The Gly-rich repeats in spidroin 2 include Gly-Pro-Gly-Gly-X and Gly-Pro-Gly-Gln-Gln (Hinmann and Lewis 1992).

This alternating pattern of hydrophilic and hydrophobic segments is important for spidroin solubility. The binding of the water molecules prevents premature crystallization. In addition, it regulates the lateral molecule aggregation that initiates the fibril formation (Oroudjev et al. 2002).

Nuclear magnetic resonance and X-ray diffraction studies revealed a high content of crystalline domains consisting of poly-A antiparallel β-sheets, packed into an orthorhombic unit cell with dimensions of at least $2 \times 5 \times 7$ nm (Warwicker 1960; Glisovic and Salditt 2007). These domains provide the tensile strength of silk fiber, while the Gly-rich matrix is responsible for the elasticity (Simmons et al. 1994; Parkhe et al. 1997; van Beek et al. 2002).

The assembly of natural spider silk fibrils starts in a spider's gland from the very concentrated (45–50%) spinning dope solution. There are two basic models that explain how the hydrophobic molecules avoid premature crystallization. The "micelle" hypothesis (Jin and Kaplan 2003) suggests that fibroin molecules stay in the highly concentrated dope by forming the micelles with hydrophobic domains on the inside and the hydrophilic termini facing the surrounding aqueous media. Dehydration and subsequent increase in protein concentration force the micelles to aggregate into globules of several micrometers in diameter. Further physical shear leads to the formation of the fibrils.

Another hypothesis (Knight and Vollrath 2002) suggests that the dope solution may have the characteristics of the liquid crystal elastomer. The folded rod-shaped spidroin molecule may be assembled into nematic units in the highly concentrated dope solution. The dehydration and increase in potassium and hydrogen ions concentration will lead to the partially unfolding of the molecules by disrupting their water shell (Chen et al. 2002; Vollrath and Knight 2001). The partially unfolded molecules extend until they are close together and form aligned segments.

The draw down taper—the last step in the silking process—causes major structural rearrangements in the proteins, resulting in rapid conversion of the aqueous dope solution into an insoluble protein filament (Vollrath and Knight 2001; Thiel et al. 1997; Knight et al. 2000). During this process, the Gly-rich parts undergo a transition from a "random coil"/β-turn/α-helical structure (Hijirida et al. 1996) to a partly β-sheet conformation and an apparently helical structure with an approximate threefold symmetry (Kümmerlen et al. 1996; van Beek et al. 2002). Despite many advanced experimental studies, the relationship

between structure and mechanical properties of silk fiber is still not well understood, in particular since the structural organization of the fibers is still somewhat controversial.

The aim of this study was to model the complete process of spider silk assembly. Special attention was given to the differences between the two recombinant analogs of spidroins 1 and 2—proteins with a primary structure that resolve to great detail the structure of the native spidroins. Using electrospinning, we were able to produce films with characteristics that are perspective for further biomedical application in fields of controlled drug release, new biomaterials, or tissue engineering.

Materials and methods

Protein expression and purification

Two artificial genes, 1f9 and 2e12, were subcloned into a methylotrophic yeast *Pichia pastoris* by integration into chromosome under the control of promoter alcohol oxidase. Proteins 1F9 and 2E12 (spidroins 1 and 2, respectively) have been purified using the cation exchange column, as described in Bogush et al (2006) with some modifications. The purified proteins were dialyzed against deionized water, lyophilized, and stored at +4°C until use.

The preparation of stock solutions of recombinant spidroins

All materials used in this study were purchased from Sigma-Aldrich. The lyophilized protein was dissolved overnight in a binary mixture (60% NaNCS water solution mixed with 20% acetate solution at the 8:2 ratio) or in 10% solution of LiCl in 90% formic acid to the concentrations of 20–30%. The protein solution was then centrifuged for 30 min to remove the insoluble debris.

Electrospinning

The existing electrospray system was used with some modifications. The capillary, made of stainless steel, has a diameter of 0.15 mm. The distance between the capillary and the supporting surface was about 20 mm. The time of the electrospray was 10 min. The voltage range was 4–7 kV. The high-oriented pyrolytic graphite and polycrystalline silicone was used as support.

Fiber formation

One to 2 µl of stock protein solutions were forced with low pressure generated by the peristaltic pump directly into the container with 96% ethanol through the specially made conical microspinneret (3–4 cm long, the output hole diameter lesser than 50 µ). The feeding speed did not exceed 0.5–1.0 µl/min. The "as spoon" filament was formed immediately, when the solution was extruded into 96% ethanol, and was allowed to fall freely and coil at the bottom of the container. Newly prepared fibers were hand-drawn twice on 25% from their initial length in an ethanol–water coagulation bath (92% and 75% ethanol) and were annealed for 20 min at 100°C without fixing the ends. The last stages include plasticization in the deionized water with hand draw on 25% from the initial length and drying on the air.

Preparation of the thin films from the stock solutions using different methods

About 1 µl of the stock solution of protein was applied to the degreased cover glass. In *shift method*, the edge of the second cover glass was used to shift this drop to produce the protein film. In *application method*, the second glass was quickly applied onto the drop and removed carefully. In *casting method*, a drop of the diluted protein solution (1 mg/ml) was applied to the fresh split mica and dried slowly (40–60 min)

All films were dried on the air for 1 min before they were submerging for 2 min into either 96% ethanol at room temperature or into a hot sodium sulfate solution (250 g/l, 45–50°C). The finished films were carefully removed from the glass and quickly rinsed in deionized water.

Atomic force microscopy analysis

Atomic force microscopy (AFM) measurements were done on a SolverBio P47 microscope (NT-MDT, Russia). AFM images were obtained in tapping mode using NSG 10 cantilevers (NT-MDT, Russia) and the high-resolution cantilevers (Nanotuning, Russia). The rate of scanning was 0.5–1.0 Hz, and the angle of scanning was 0–90°. All images were obtained in air with uncontrolled humidity of surrounding air. A drop (10 µl) of the diluted water solution of protein (1 mg/ml) was deposited on the freshly cleaved mica surface. After 10 min adsorption, the surface was washed with drops of water and dried with a stream of argon.

Infrared spectra

Infrared (IR) spectra were obtained in 4,000–1,300 cm^{-1} range by Magna-750 (Nicolet, USA) IR-Fourier-spectrometer. The following bands were included in the measurements: amide I, amide II, amide A, and amide B.

Circular dichroism spectra

Circular dichroism (CD) spectra were recorded on Jasco J-715 (Jasco, Japan) spectropolarimeter equipped with

Peltier-type temperature control system PTC-423S/L (Jasco, Japan).

Scanning electron microscopy analysis

The morphology of films was observed using a scanning electron microscope (SEM) Camscan S2 (Cambridge Instruments, UK). The untreated dry samples, attached to double-sided adhesive conductive tape (SPI, USA) were sputter-coated with gold using the ion coater IB-3 (Eico, Yapan) and observed in the microscope at two magnifications: ×1,160 and ×2,430 to obtain the general and detailed pictures of the sample. The images were captured using the software MicroCapture (SMA, Russia).

Transmission electron microscopy analysis

The 0.1 mg/ml water solution of lyophilized protein was applied to a glow-discharged carbon-coated copper grid and subjected to a 2% uranyl acetate solution for 30 s. Grids were examined in a FEI Tecnai G12 electron microscope (FEI, Hillsboro, OR, USA) at 120 kV under low-dose conditions. Images were taken at a magnification of ×52,000 and 1.5–1.8 μm underfocus. The negatives were digitized on a Nikon COOLSCAN 9000 scanner (Nikon, USA).

Molecular dynamics simulations

Molecular dynamics (MD) simulations for signal peptides and stacks of peptides in viscous medium were carried out. GROMAX software with OPLS-AA force field (Cornell et al. 1995) was used for MD simulations (Berendsen et al. 1995). Total systems were minimized and equilibrated for 100 ps, then equilibrium MD simulation was made using the following MD protocol: time step—1 fs; total trajectory length—10 ns; temperature coupling—berendsen, stochastic dynamics; system temperature—300 K; time constant for coupling—0.5 ps; coulomb cutoff—2 nm; and van der Waals cutoff—2 nm. The steered MD experiments additionally included the external force of 1, 2, 3, 4, 5, and 10 kcal/(mol Å).

Results

Designing the primary structure of analogs of spidroins 1 and 2

The periodical patterns of the fibrous proteins define their physical–chemical characteristics, the secondary structure, and the fibril packing (Parkhe et al. 1997). In an engineered protein, we decided to reproduce the periodic patterns observed in natural spider silk, especially their unique amino acid structure.
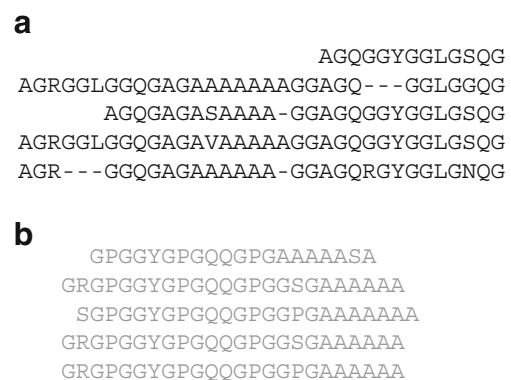
Analog of spidroin 1

The structure of the artificial spider gene was designed on the basis of the known nucleotide sequence of corresponding cDNA from *Nephila clavipes* (Xu and Lewis 1990). Four fragments encoding repeated units were chosen from the sequence of the native protein. They are the most typical repeated units for this type of spider protein. These segments differ by the set of deletions in the amino acid sequence. The designed DNA fragment includes approximately 400 base pairs and encodes the polypeptides corresponding to 134 amino acid residues. The "rare" codons in the sequence of the artificial gene were substituted by the most frequent codons, characteristic for the codon usage of *P. pastoris*. The designed amino acid sequence is presented in Fig. 1a.

The monomer was synthesized by chemical–enzymatic gene synthesis and the multimeric form of the artificial gene was obtained using a step-by-step duplication of the monomer in the recombinant plasmid in Escherichia *coli* at the restriction sites BamHI and BglII (Bogush et al. 2001). The resulting multimeric gene contains nine copies of monomers. This gene encodes the spidroin 1 analog, named 1F9, with the molecular mass of 94 kDa.

Analog of spidroin 2

The National Center for Biotechnology Information (NCBI) protein database (SwissProt + TrEmbl) contains a long fragment (about 2,000 residues) of *Nephila madagascariensis* spidroin-2 sequence. We used this sequence to find specific periodical patterns, determined by characteristic combinations of symbols. All sequences of spidroins, longer than 200 residues, and presented in the NCBI protein database were examined. We used symbolic Fourier transform algorithm implemented in the SymFour (Makeev and Tumanyan 1996) and Catseq (Ragulina et al. 2004) programs. Basing on the sequence analysis

a

```
                 AGQGGYGGLGSQG
AGRGGLGGQGAGAAAAAAAGGAGQ---GGLGGQG
        AGQGAGASAAAA-GGAGQGGYGGLGSQG
AGRGGLGGQGAGAVAAAAAGGAGQGGYGGLGSQG
AGR---GGQGAGAAAAAA-GGAGQRGYGGLGNQG
```

b

```
   GPGGYGPGQQGPGAAAAASA
 GRGPGGYGPGQQGPGGSGAAAAAA
  SGPGGYGPGQQGPGGPGAAAAAA
 GRGPGGYGPGQQGPGGSGAAAAAA
 GRGPGGYGPGQQGPGGPGAAAAAA
```

Fig. 1 Aligned amino acid sequences of "monomers" of 1F9 (**a**) and 2E12 (**b**) used for design of the artificial gene structure

of natural spidroin 2 of *N. madagascariensis*, the sequences of blocks (each block consist of three to five initial repeats) and corresponding formula for the whole artificial protein were developed: ABACA[DBCDA$_2$][DBCDE$_2$]D$_2$BF. Comparison of the Fourier spectra of the designed sequence with that of the native sequence indicates that the basic periodic patterns mainly retained in the designed sequence (for both the whole sequence and each of its domains).

As a result, one of the variants of the native gene consensus sequence, a poly-E gene (the E-block), was synthesized (Fig. 1b) that is identical to one of the basic areas of native spidroin 2. To overcome the problem of gene instability caused by direct repeats, an improved method for synthesis was developed. The gene was obtained by annealing and simultaneous ligation of seven variants of the mono-E gene (each variant was synthesized using different oligonucleotides by degeneracy of the genetic code). Finally, the artificial gene 2e12, the analog of gene that codes the spidroin 2, was obtained, containing 12 repeated E-blocks with a total length of 4.2 kb and encoding the 2E12 protein with the molecular weight of 113 kDa.

Molecular modeling

Molecular modeling was used to determine the preferable secondary structures of known repeats, from different fibrous proteins: the poly-Ala peptide (four, eight, and 12 repeats), the intermediate peptide from *N. clavipes* spidroin-1 (GGAGG GYGGLGSQGAGRGGQG), and poly-AG peptide from *B. mori*. The β-sheet was chosen as the initial conformation of the peptide. Experiments on single peptides demonstrated that all three types of peptides do not retain the original conformation, yet prefer a helical conformation. However, the stacks consisting of five peptides remained stable and partially preserved the original β-sheet conformation. The peptide elongation correlates with the increase in β-sheet content. We concluded that the full-size spidroin molecules are ready to self-organize into fibrils.

To measure the flexibility of stacks, built from different peptides, we used the steered molecular dynamics. The N-termini of peptides were experimentally fixed and the various external forces applied. We demonstrated that the intermediate peptide of spidroin 1 exhibits the maximal relative elongation, while the poly-Ala peptides exhibited the minimal elongation. We concluded that the intermediate peptides might be responsible for the flexibility of the fibrils.

Circular dichroism

To assess the characteristic features of conformational transitions in spidroins 1 and 2, the CD spectra of diluted solutions of recombinant proteins 1F9 and 2E12 were studied. After adding the 50% ethanol or vortexing for 1.5 min, the CD spectra of the 2E12 protein solution (Fig. 2e) develop the minimum at 190 nm and the maximum at 220 nm. The secondary structure of PPII type was predominant in 0.1 mg/ml solutions, whereas the mixture of β-structure and PPII was characteristic for 0.5 mg/ml solutions. Most of the molecules in 1 mg/ml solutions adopt a β-structural conformation. Notably, the isobestic point was present in all cases and retains its position, which indicates that the transition involves only two states, the PPII and the β-structure.

Nanofibrils formation

The self-assembly of spidroins leads to the formation of nanofibrils (Knight and Vollrath 2002; Oroudjev et al. 2002). In our experiments, both purified recombinant analogs of spidroins spontaneously form nanofibrils in aqueous solutions (Fig. 2a,b). The nanofibrils observed by AFM were from 2.5 to 5 nm in height (Fig. 3b) with the variable length that differs from 200 nm to 1 μm. We demonstrated a different ability to form nanofibrils in solution for 1F9 and 2E12 proteins. The 1F9 self-assembles to longer nanofibrils (up to 1 μm in total length) with the persistent length of 330±30 nm (Fig. 2a), at the concentration as low as 0.1 mg/ml. The 2E12 possesses a tendency to produce shorter and less flexible nanofibrils (200–700 nm in total length with the persistent length 560±80 nm; Fig. 2b). Interestingly, following the storage at room temperature for a week, the nanofibrils became shorter and a number of round globules with a diameter of about 1 μm appeared. Although we observed the globules, associated with nanofibrils more often, the somewhat larger aggregates were also present, especially in solutions, containing 10–50% of ethanol.

Following the lyophilization and dissolving in deionized water, a binary mix or guanidine HCl, nanofibrils were still present. They disappeared only after dissolving of the proteins in the LiCl solution (see "Materials and methods", data not shown), apparently because of the complete unfolding of the protein under these conditions. This fact suggests that the nanofibril resembles a native quaternary structure of a protein rather than it is an artifact caused by the interactions between protein and the substrate.

The high-resolution AFM revealed the periodic substructure of nanofibrils (Fig. 3a) with the 40 nm repeating motif in the high profile (Fig. 3b). A similar periodic substructure was observed before by the AFM methods and was shown to be characteristic for the nanofibrils (Oroudjev et al. 2002). To obtain a more detailed picture of a nanofibril and to understand the nature of its periodicity, we employed the transmission electron microscopy (TEM) and negative staining. This method was successfully used

Fig. 2 Polymorphism in nano-fibril morphology. An AFM image of nanofibrils in aqueous solutions of **a** 1F9 (*C*=0.1 mg/ml) and **b** 2E12 (*C*=1.4 mg/ml), mount on mica. The AFM images of electrospun nanofibrils of **c** 8% solution of protein 1F9 and **d** 6% solution of protein 2E12 in fluoro-2-propanol; **e** CD spectra of 2E12 in the aqueous solution (*C*=0.1 mg/ml). *Solid line* 24 h storage; *dotted line* after addition of 50% ethanol; *dashed line* after vortex shaking for 1.5 min. The *bar* size is 1 μm
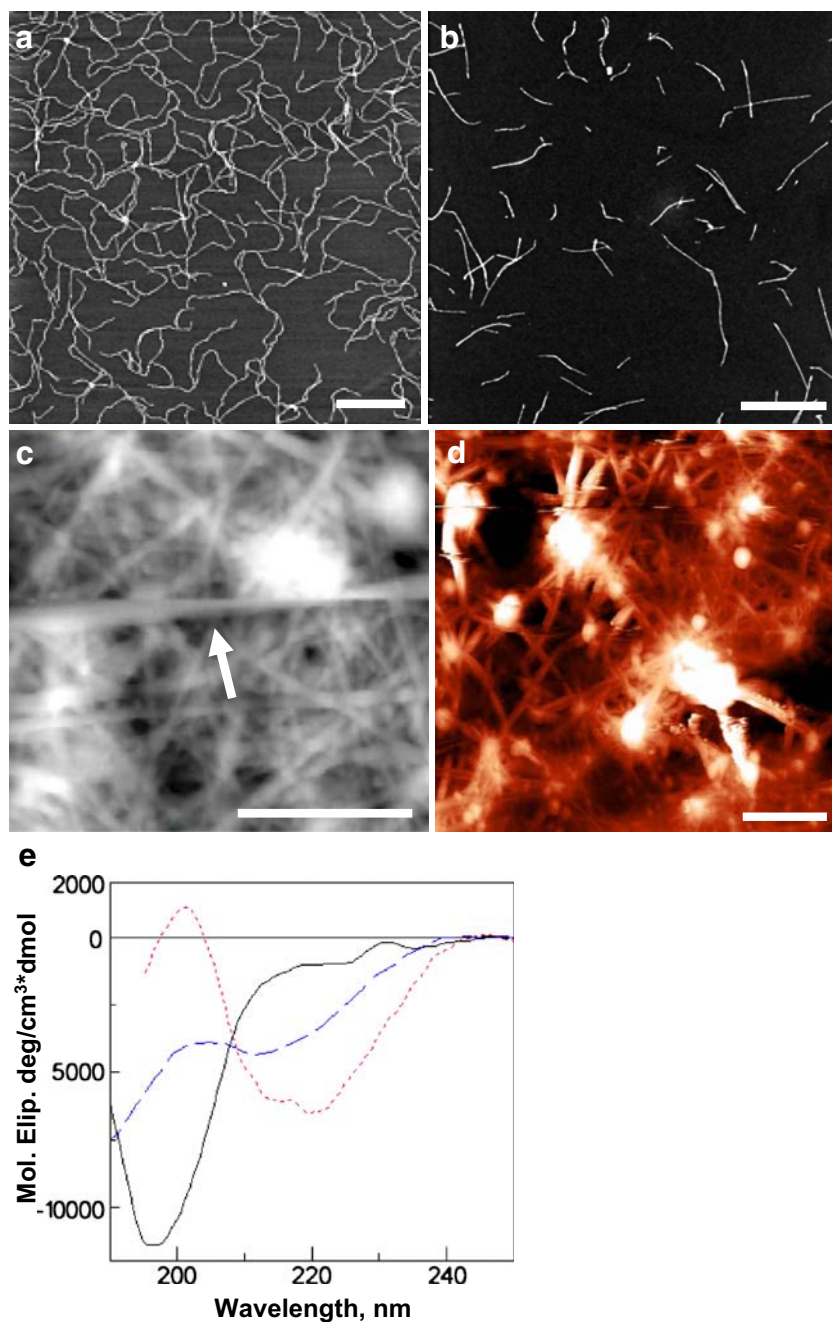
before to observe the nanofibrils in the diluted solution of spider dope (Chen et al. 2002) and amyloid fibrils from insulin (Jimenez et al. 1999), SH3-domain (Jimenez et al. 2002), and Alzheimer peptide (Sachse et al. 2006). In our experiments, the nanofibrils formed by 1F9 protein revealed the linear structure with varying thickness of about 13 nm in thicker parts and about 5 nm in crossovers (Fig. 3c). We think that these crossovers reflect a periodic helical twist of the overall fibril structure with the periodicity of about 40 nm, which is consistent with our AFM data.

Electrospinning

In the past decade, the method of electrospinning emerged as an attractive method of producing the nanofibrils from both natural (Kim et al. 2005; Matthews et al. 2002) and synthetic polymers (Li et al. 2002; Zong et al. 2002). In the present study, we employed this method to obtain nano-fibrils from proteins, analogs of spidroins 1 and 2. We have been able to obtain thin nanofibrils with diameters of 10 to 400 nm from the protein 1F9 dissolved in fluoro-2-propanol (concentration used was 4% to 8%). The typical
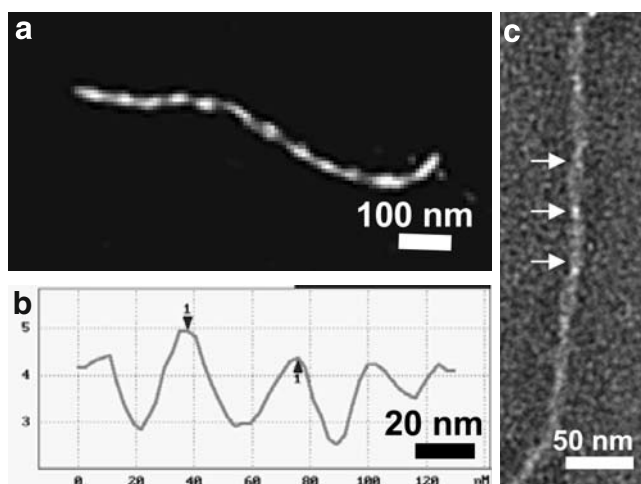
Fig. 3 The amyloid-like properties of the nanofibrils. **a** The high-resolution AFM image of nanofibril formed by 1F9 protein. **b** The height profile of the nanofibril in **a**. *Arrows* are pointing to the repeating motif along the nanofibril. **c** EM image of the negatively stained nanofibril formed by 1F9. *Arrows* are marking the periodic twists of the overall fibril structure

structure of the electrospun nanofibrils of the protein 1F9, forming the dense mesh on the surface, is depicted on the Fig. 2c. Most of the nanofibrils look like thin bands with lengths that exceed 1 mm. The characteristic twist of the band in the Fig. 2c is marked with an arrow. This twist resembles one of the periodical twists of the nanofibril in solution (Fig. 3c), although the electrospun fibril is much larger (200 nm wide and about 20 nm thick). As a result of the electrospinning of the 6% 2E12 solution in fluoro-2-propanol, the shorter nanofibrils (thickness was more than 600 nm) with a somewhat intricate structure were obtained (Fig. 2d).
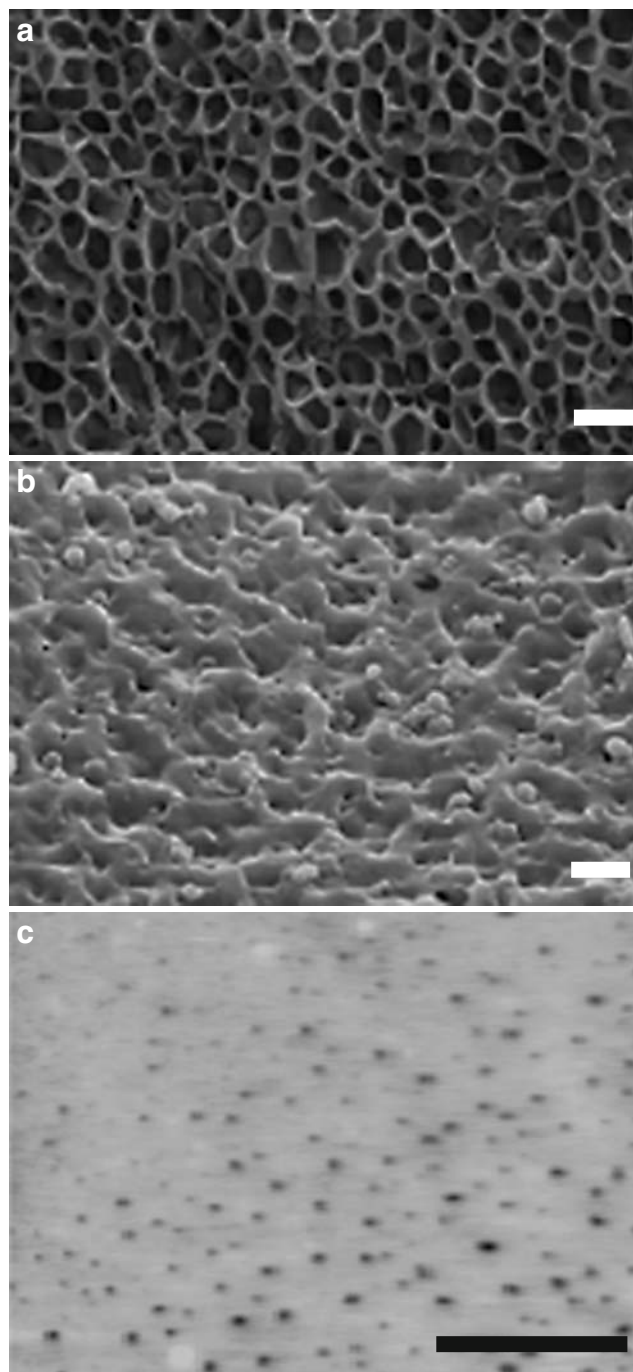
Thin films

Both recombinant analogs of spidroins 1 and 2 possess the ability to form thin films. We prepared thin films that were attached to glass or graphite using different methods: application, casting, and shift (see "Materials and methods" section).

The morphology of thin films, prepared using application and shift methods, is somewhat similar: they possess a rough surface with a large number of pores. All films have the thickness of 1–3 μm. The average pore size in films prepared using application (Fig. 4a) and shift (Fig. 4b) method was as little as 1 and 3 μm, respectively. The larger pore size correlates to some extent with the higher protein concentration. Films, prepared by the casting method (Fig. 4c) have smoother surface with the pores of much smaller diameter: from 100 to 250 nm for protein 1F9 and from 40 to 80 nm for 2E12.

IR spectra

The thin films prepared by methods of electrospinning and casting were studied using the Fourier transform infrared (FTIR) analysis. We compared the structure of films obtained from protein 2E12 with the films and obtained

Fig. 4 The morphology of thin films prepared using different methods. SEM images of films cast from a 25% solution of 1F9 in sodium rhodanate, using the application (**a**), shift (**b**), and casting (**c**) methods and subsequent treatment with 96% ethanol. The bar size is 3 μm

from the mixture of the two proteins 2E12 and 1F9 at 1:1 and 1:2 ratios. In all cases, the spectra were similar to the spectrum of pure 2E12 proteins. The components frequencies observed in variety of samples coincided to the mixture of parallel and antiparallel β-sheet structures. The antiparallel β-sheet structure was prominent in the spectra of the films obtained by electrospinning. In contrast, the absence of a band above 1,680 cm^{-1} suggests the parallel disposition of β-strands (Hiramatsu et al. 2005) in the films prepared by the casting method.

Synthetic silk spinning

The last part of our work was dedicated to the study of properties of recombinant spidroins 1 and 2 spin solutions. Our aim was to evaluate their spinning potential and optimal conditions for fiber formation.

We have developed an improved scheme for synthetic fiber formation: (a) spinning into bath with ethanol, (b) stretching (including two stages), (c) annealing, (d) plasticization, and (e) drying. After processing, the synthetic fibers kept elasticity of 5% to 15%, comparable to the typical values known for the native fibers. They exhibited a relative tensile strength: 0.1–0.15 GPa. This value is comparable to the previous results, obtained for the recombinant spidroin 1 (0.14 GPa; Fahnestock 1994) and is two times less than the value for the regenerated *N. clavipes* silk (0.32 GPa; Seidel et al. 2000).

Discussion

In vivo, the spinning solution undergoes a maturation stage with a subsequent transformation of the pre-oriented liquid crystalline solution into a rigid dragline thread that occurs during the very fast draw down. This process includes several coordinated acts, such as the formation of liquid crystalline from protein solution, molecular orientation and alignment, dehydration, the removal of sodium and chloride ions and the introduction of potassium ions, acidification of the dope to pH 6.3, transition of coil and α-spiral structures into β-sheet structures, and formations of β-sheets. Most of these processes take place in the distal part of the third limb of the duct (Knight and Vollrath 2001). Since the subjects of our investigation are recombinant analogs of spidroins, we intend to model and study these processes separately.

As it was demonstrated earlier, the high mechanical performance of spider dragline silk is probably due to the β-sheet conformation of poly-Ala domains, embedded as small crystallites within the fiber (Yang et al. 1997; van Beek et al. 2002). Our molecular dynamics experiments demonstrated that the poly-A peptides were the most durable parts of spidroins, comparing to the intermediate

peptide (the sequence that connects the poly-A domains and may be variable along the protein) and poly AG. Moreover, the poly-A peptides possess a tendency to form a hyper-helical structure, while the intermediate peptide was mainly unstructured. According to our present and previous (Simmons et al. 1994; Parkhe et al. 1997; van Beek et al. 2002) studies, the inner Gly-rich peptide is responsible for the elasticity of the fibers. Thus, by altering the poly-A peptides (durable but not flexible) and intermediate peptides (flexible, but not durable), we can design the analogs of spidroins with adjusted mechanical properties.

The artificial gene sequences of spidroin 1 and 2 have been designed using computer analysis of existing databases and mathematical modeling (see "Results"). Two artificial genes, coding the analogs of the core regions of natural spidroins 1 and 2, have been generated by amplification of the synthesized monomers (see "Materials and methods"). Both constructs do not include the hydrophilic N- and C-termini. The synthesis of the whole artificial gene appears to be a very complex problem, which will be solved during further experiments. Some authors (Jin and Kaplan 2003; Ittah et al. 2006) suggested that hydrophilic N- and C-termini are necessary for nanofibril's and micelle's formation. Nevertheless, the proteins obtained from expression of the artificial genes that contain only the hydrophobic core regions possess all characteristic properties of the full-length spidroins. In solution, they produce the nanofibrils (Fig. 2a,b) and after spinning into alcohol form strong fibers.

The formation of nanofibrils is one of the most apparent indications that the proteins are capable for self-assembly. Nanofibrils with similar dimensions have been observed in the solutions of recombinant spidroin analogs (Oroudjev et al. 2002; Chen et al. 2002; Slotta et al. 2007) and amiloids (Slotta et al. 2007). Nanofibrils have also been observed in the diluted dope solution from the distal part of a spider gland (Kenney et al. 2002; Du et al. 2006). The most extensively used method to observe the nanofibril formation by spidroins was, until recently, the AFM (Chen et al. 2002; Oroudjev et al. 2002; Slotta et al. 2007). However, the resolution of the conventional AFM method is limited by the cantilever tip size (usually 5–10 nm). In the present study, we employed the high-resolution AFM (using the high-resolution cantilevers with the tip size of about 1 nm) and TEM together with negative staining to discover for the first time a helical structure of nanofibrils with a repeating motif every 40–50 nm (Fig. 3). In the previous studies (Oroudjev et al. 2002), the segmented structure of the nanofibrils was also reported. Our findings suggest that the previously observed segments were actually helix cross-overs, similar to those found in the amyloid fibrils (Jimenez et al. 1999, 2002; Sachse et al. 2006). The further experiments, including the precise measurement of the

morphological and kinetic parameters, as well as the comparative studying of different recombinant spidroin analogs are required to decipher the exact mechanism of nanofibril formation.

The electrospinning—a recently discovered method—is capable of producing nanofibrils of a larger size: with the diameter of 2 to 1,000 nm. The potential applications of this method include mimicking the natural extracellular matrix (Xu et al. 2004), tissue engineering scaffolds, nanocomposite reinforced fibers (Jayaraman et al. 2004), and filtration of nanoparticles in vivo. In the present study, we were able to produce electrospun nanofibrils that form thin films with the antiparallel β-structure on the surface of modified graphite (Fig. 2c,d) as was shown by the FTIR analysis. The FTIR is decisive in respect to the type of β-sheet structure; in particular, the amid I band is especially informative in determination whether parallel or antiparallel structure is realized in the sample (Hiramatsu et al. 2005).

To study the secondary structure formation within these films, we used a variety of sample preparation techniques, solvents (sodium rhodanate-acetic acid or LiCl-formic acid) and ways to dehydrate the sample. An alteration of water structure in recombinant spidroin solutions by ethanol results in a structural transition from the PPII structure to the β-sheet structure. The concentration dependence of these transitions in recombinant spidroin can indicate the intermolecular interactions. Vortex shaking also causes a drastic change in the conformation (Fig. 2e, dashed line) and can thus be regarded as an analog of the hydrodynamic shift.

In summary, we developed a novel model system that includes two recombinant analogs of spidroins 1 and 2 (Fig. 5). This model system resembles all basic processes that occur during the web spinning by spiders in vivo. To obtain the spinning solution, the recombinant proteins were dissolved in concentration of more than 25%, similar to the natural spider dope. The use of ethanol for precipitation is comparable to the process of water removal from dope solution by the reversed osmosis in the spider gland (Kenney et al. 2002). The structural transitions in recombinant spidroins and their supramolecular structures (threads, films, nanofibrils) that can be induced in vitro were also similar to those found in natural spidroins.

We also presented new evidence of the structural similarities between nanofibrils and amyloids. Taking into account the fact that the spider fibril formation, similar to amyloid, requires a nucleation step (Li et al. 2001), our model system could be employed for the study of amyloid formation.

Finally, by altering the primary structure of the proteins and/or the processing conditions, one could design materials and matrices with determined quaternary structure and targeted mechanical properties that could be used for various

Fig. 5 The spidroin model system and its biomedical applications
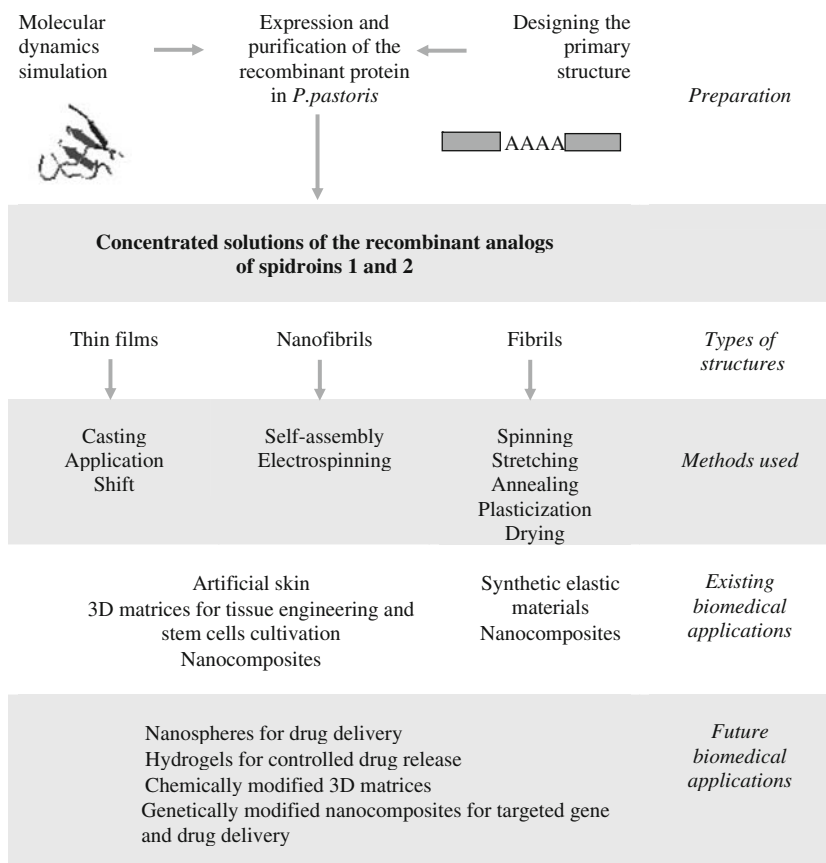
biomedical applications, such as tissue engineering and drug delivery.

References

Ayutsede J, Gandhi M, Sukigara S, Micklus M, Chen H-E, Ko F (2005) Regeneration of *Bombyx mori* silk by electrospinning. Part 3: characterization of electrospun nonwoven mat. Polymer (Guildf) 46:1625–1634. doi:10.1016/j.polymer.2004.11.029

Berendsen HJC, Van der Spoel D, Van Drunen R (1995) GROMACS: a message-passing parallel molecular dynamics implementation. Comput Phys Commun 95:43–56. doi:10.1016/0010-4655(95)00042-E

Bogush VG, Sidoruk KV, Molchan OK, Ptitsyn LR, Altman IB, Kozlov DG et al (2001) The molecular cloning and expression in yeast of synthetic genes encoding the protein analogs of dragline silk protein spidroin 1. Biotekhnologiya 2:11–22

Bogush VG, Sazykin AY, Davydova LI, Martirosyan VV, Sidoruk KV, Glazunov AV et al (2006) Obtaining, purification and silking of recombinant analog of spidroin 1. Biotechnologiya 4:3–12

Chen X, Knight DP, Vollrath F (2002) Reological characterization of *Nephila* spidroin solution. Biomacromolecules 3:644–648. doi:10.1021/bm0156126

Cornell WD, Cieplak P, Bayly CI (1995) A second generation force field for the simulation of proteins, nucleic acids and organic molecules. J Am Chem Soc 117:5179–5197. doi:10.1021/ja00124a002

Cunniff PM, Fossey SA, Auerbach MA, Song JW, Kaplan DL, Adams WW et al (1994) Mechanical and thermal properties of dragline silk from the spider, *Nephila clavipes*. Polym Adv Technol 5:401–410. doi:10.1002/pat.1994.220050801

Du N, Liu XY, Narayanan J, Li L, Lim ML, Li D (2006) Design of superior spider silk: from nanostructure to mechanical properties. J Biophys 91(12):4528–4535. doi:10.1529/biophysj.106.089144

Fahnestock SR (1994) Novel, recombinantly produced spider silk analogs. Int Application # PCT/US94/06689, Int Publication # WO 94/29450

Fang J-Y, Chen J-P, Leu Y-L, Wang H-Y (2006) Characterization and evaluation of silk protein hydrogels for drug delivery. Chem Pharm Bull (Tokyo) 54(2):156–162. doi:10.1248/cpb.54.156

Feng X-X, Zhang L-L, Chen J-Y, Guo Y-H, Zhang H-P, Jia C-I (2007) Preparation and characterization of novel nanocomposite films formed from silk fibroin and nano-TiO2. Int J Biol Macromol 40:105–111. doi:10.1016/j.ijbiomac.2006.06.011

Furuzono T, Kishida A, Tanaka J (2004) Nano-scaled hydroxyapatite/polymer composite. J Mater Sci 15:19–23. doi:10.1023/B:JMSM.0000010093.39298.5a

Glisovic A, Salditt T (2007) Temperature dependent structure of spider silk by X-ray diffraction. Appl Phys A 87:63–69.

Hijirida DH, Do KG, Michal C, Wong S, Zax D, Jelinski LW (1996) C13 NMR of *Nephila clavipes* major ampullate silk gland. J Biophys 71:3442–3447

Hinman MB, Lewis RV (1992) Isolation of a clone encoding a second dragline silk fibroin. J Biol Chem 267:19320–19324

Hiramatsu H, Goto Y, Naiki H, Kitagava T (2005) Structural model of the amyloid fibril formed by β2-microglobulin #21–31 fragment based on vibrational spectroscopy. J Am Chem Soc 127:7988–7989. doi:10.1021/ja050844o

Hoffman S, Po Foo S-TW, Rossetti F, Textor M, Vunjak-Novakovic G, Kaplan DL et al (2007) Silk fibroin as an organic polymer for controlled drug delivery. Biomaterials 28(6):1152–1162. doi:10.1016/j.biomaterials.2006.10.019

Ittah S, Cohen S, Garty S, Cohn D, Gat U (2006) An essential role for the c-terminal domain of a dragline spider silk protein in directing fiber formation. Biomacromolecules 7:1790–1795.

Jayaraman K, Kotaki M, Zhang Y, Mo X, Ramakrishna S (2004) Recent advances in polymer nanofibers. J Nanosci Nanotechnol 4(1/2):52–65

Jimenez JL, Guijarro JI, Orlova E, Zurdo J, Dobson CM, Sunde M, Saibil HR (1999) Cryoelectron microscopy structure of an SH3 amyloid fibril and model of the molecular packing. EMBO J 18:815–821.

Jimenez JL, Nettleton EJ, Bouchard M, Robinson CV, Dobson CM, Saibil HR (2002) The protofilament structure of insulin amyloid fibrils. Proc Natl Acad Sci U S A 99:9196–9201. doi:10.1073/pnas.142459399

Jin H-J, Kaplan DL (2003) Mechanism of silk processing in insects and spiders. Nature 424:1057–1061. doi:10.1038/nature01809

Katti DS, Robinson KW, Ko FK, Laurencin CT (2004) Bioresorbable nanofiber-based systems for wound healing and drug delivery: optimization of fabrication parameters. J Biomed Mater Res 70B(2):286–296. doi:10.1002/jbm.b.30041

Kenney JM, Knight D, Wise MJ, Vollrath F (2002) Amyloidogenic nature of spider silk. Eur J Biochem 269:4159–4163. doi:10.1046/j.1432-1033.2002.03112.x

Kim K-H, Jeong L, Park H-N, Shin S-Y, Park W-H, Lee S-C et al (2005) Biological efficacy of silk fibroin nanofiber membranes for guided bone regeneration. J Biotechnol 120:327–339. doi:10.1016/j.jbiotec.2005.06.033

Knight DP, Vollrath F (2001) Comparison of the spinning of Selachian egg case ply sheets and orb web spider dragline filaments. Biomacromolecules 2:323–334 . doi:10.1021/bm0001446

Knight DP, Vollrath F (2002) Spinning an elastic ribbon of spider silk. Philos Trans R Soc Lond B Biol Sci 357(1418):219–227. doi:10.1098/rstb.2001.1026

Knight DP, Knight MM, Vollrath F (2000) Beta transition and stress-induced phase separation in the spinning of spider dragline silk. Int J Biol Macromol 27:205–210. doi:10.1016/S0141-8130(00)00124-0

Kümmerlen J, van Beek J, Vollrath F, Meier B (1996) Local structure in spider dragline silk investigated by two-dimensional spin-diffusion nuclear magnetic resonance. Macromolecules 29:2920–2928

Li G, Zhou P, Shao Z, Xie X, Chen X, Wang H et al (2001) The natural silk spinning process. A nucleation-dependent aggregation mechanism? Eur J Biochem 268:6600–6606. doi:10.1046/j.0014-2956.2001.02614.x

Li WJ, Laurencin CT, Caterson EJ, Tuan RS, Ko FK (2002) Electrospun nanofibrous structure: a novel scaffold for tissue engineering. J Biomed Mater Res 60:613–621. doi:10.1002/jbm.10167

Makeev VJu, Tumanyan VG (1996) Search of periodicities in primary structure of biopolymers: a general Fourier approach. Comput Appl Biosci 12:49–54

Matthews JA, Wnek GE, Simpson DG, Bowlin GL (2002) Electro-spinning of collagen nanofibers. Biomacromolecules 3(2):232–238. doi:10.1021/bm015533u

Min B-M, Jeong L, Nam YS, Kim J-M, Kim JY, Park WH (2004) Formation of silk fibroin matrices with different texture and its cellular response to normal human keratinocytes. Int J Biol Macromol 34:223–230. doi:10.1016/j.ijbiomac.2004.08.004

Oroudjev E, Soares J, Arcidiacono S, Thompson JB, Fossey SA, Hansma HG (2002) Segmented nanofibers of spider dragline silk: atomic force microscopy and single-molecule force spectroscopy. Proc Natl Acad Sci U S A 99(2):6460–6465. doi:10.1073/pnas.082526499

Parkhe AD, Seeley SK, Gardner K, Thompson L, Lewis RV (1997) Structural studies of spider silk proteins in the fiber. J Mol

Recognit 10:1–6. doi:10.1002/(SICI)1099-1352(199701/02)
10:1<1::AID-JMR338>3.0.CO;2-7

Po Foo CW, Patwardhan SV, Belton DJ, Kitchel B, Anastasiades D, Huang J et al (2006) Novel nanocomposites from spider silk–silica fusion (chimeric) proteins. Proc Natl Acad Sci U S A 103 (25):9428–9433. doi:10.1073/pnas.0601096103

Ragulina LE, Makeev VJu, Esipova NG, Tumanyan VG, Nikitin VG, Bogush VG, Debabov VG (2004) Study of periodicity in primary structure of spidroin 1 and spidroin 2 of spiders belonging to various species. Biophysika 49:1053–1060

Sachse C, Xu C, Wieligmann K, Diekmann S, Grigorieff N, Fändrich M (2006) Quaternary structure of a mature amyloid fibril from Alzheimer's Abeta(1–40) peptide. J Mol Biol 262(2):347–354. doi:10.1016/j.jmb.2006.07.011

Seidel A, Liivak O, Calve S, Adaska J, Ji G, Yang Z et al (2000) Regenereted spider silk: processing, properties and structure. Macromolecules 33:775–780. doi:10.1021/ma990893j

Simmons AH, Ray E, Jelinski LW (1994) Solid-state ^{13}C NMR of *Nephila clavipes* dragline silk establishes structure and identity of crystalline regions. Macromolecules 27:5235–5237. doi:10.1021/ma00096a060

Slotta U, Hess S, Spieß K, Stromer T, Serpell L, Scheibel T (2007) Spider silk and amyloid fibrils: a structural comparison. Macromol Biosci 7(2):183–188. doi:10.1002/mabi.200600201

Tamada Y (2005) New process to form a silk fibroin porous 3-D structure. Biomacromolecules 6:3100–3106

Thiel BL, Guess KB, Viney C (1997) Non-periodic lattice crystals in the hierarchical microstructure of spider (major ampullate) silk.

Biopolymers 41:703–719. doi:10.1002/(SICI)1097-0282 (199706)41:7<703::AID-BIP1>3.0.CO;2-T

van Beek JD, Hess S, Vollrath F, Meier BH (2002) The molecular structure of spider dragline silk: folding and orientation of the protein backbone. Proc Natl Acad Sci U S A 99:10266–10271. doi:10.1073/pnas.152162299

Vehoff T, Glisović A, Schollmeyer H, Zippelius A, Salditt T (2007) Mechanical properties of spider dragline silk: humidity, hysteresis, and relaxation. Biophys J 93(12):4425–4432. doi:10.1529/biophysj.106.099309

Vollrath F, Knight DP (2001) Liquid crystalline spinning of spider silk. Nature 410:541–548. doi:10.1038/35069000

Warwicker JO (1960) Comparative studies of fibrous. II. The crystal structure of various fibroins. J Mol Biol 2:350–362

Xu M, Lewis R (1990) Structure of a protein superfiber: spider dragline silk. Proc Natl Acad Sci U S A 87:7120–7124. doi:10.1073/pnas.87.18.7120

Xu C, Inai R, Kotaki M, Ramakrishna S (2004) Electrospun nanofiber fabrication as synthetic extracellular matrix and its potential for vascular tissue engineering. Tissue Eng 10(7/8):1160–1168. doi:10.1089/ten.2004.10.1160

Yang Z, Grubb DT, Jelinski LW (1997) Small-angle X-ray scattering of spider dragline silk. Macromolecules 30:8254–8261. doi:10.1021/ma970548z

Zong X, Kim K, Fang D, Ran S, Hsiao BS, Chu B (2002) Structure and properties of electrospun PLLA single nanofibres. Polymer (Guildf) 43:4403–4412. doi:10.1016/S0032-3861(02)00275-6